Direct Observation of the Fermi Surface in $Ba_{1-x}K_xBiO_3$

W. D. Mosley,[1,2] J. W. Dykes,[1,2] R. N. Shelton,[1] P. A. Sterne,[1,2] and R. H. Howell[2]
[1]*Department of Physics, University of California, Davis, California 95616*
[2]*Lawrence Livermore National Laboratory, Livermore, California 94550*
(Received 15 February 1994)

Positron angular correlation measurements have been used to measure electron-positron momentum density distributions in high-quality single crystals of the 32 K superconductor $Ba_{1-x}K_xBiO_3$. Using first-principles calculations we are able to separate those features due to the strong overlap of the electron and positron wave functions from those associated with Fermi surface breaks. We have identified a roughly cubic Fermi surface centered around Γ, whose location is in excellent correspondence with that predicted by the band structure calculations.

PACS numbers: 71.25.Hc, 74.72.Jt, 78.70.Bj

Recent experiments on the electronic structure of high-T_c oxide superconductors have revealed highly symmetric Fermi surface structures that may be intrinsically related to their strong electron correlation properties [1–7]. Research has primarily focused on cuprate superconductors because of their high transition temperatures. The highest T_c in a copper-free oxide material occurs at 32 K in the $Ba_{1-x}K_xBiO_{3-y}$ (BKBO) system for $x \approx 0.4$ and full oxygenation [8]. From analysis of transport and magnetic properties, BKBO appears to be an intermediate-coupling, BCS-like superconductor, but the exact nature of the coupling is still unclear. BKBO also exhibits interesting structural phase transitions which sensitively depend upon system doping levels [9]. It has been proposed that these transitions may be Fermi surface driven, but the Fermiology of an oxide with Ba/K sublattice alloying is not established [10]. Indeed, the existence of a Fermi surface in BKBO and its correspondence with band structure calculations are substantive issues.

In this paper we report results from a detailed experimental and theoretical study of the Fermi surface properties of BKBO, a structural analog to the copper-oxide superconductors. Electron-positron momentum distributions have been measured to high statistical precision in a two-dimensional positron angular correlation of annihilation radiation (2D-ACAR) apparatus. In some samples, we have found strong features resulting from electron-positron wave-function overlap and identified discontinuities in momentum space consistent with the presence of a Fermi surface. First-principles linear muffin tin orbital (LMTO) calculations were used to help distinguish Fermi surface contributions from the stronger features due to the spatial distribution of the electron and positron wave functions. The locations of the observed momentum density features are in excellent agreement with those predicted by theory. The most significant result, however, is the direct identification of a Fermi surface of high symmetry whose geometry is in quantitative agreement with theory. Direct observation of this Fermi surface provides support for theories which attribute the structural phase transition and superconductivity in the BKBO system to specific characteristics of Fermi surface features.

Single crystals of BKBO were grown using an electrochemical deposition technique [11] only slightly modified from that reported by Norton [12]. Large crystals are necessary to maximize counting rates in the positron experiment, and this synthesis yields well faceted mosaics of individual BKBO crystals, all with nearly the same orientation. The samples were not treated as air sensitive, though some surface degradation has been observed after removal from the molten KOH growth bath. The grains involved in this experiment average 2 mm × 3 mm on the growth [110] face. Refinement of x-ray diffraction data on these samples was based on previous results from neutron scattering [13] and yielded a lattice parameter of 4.29 Å with a potassium doping of $x = 0.41$. Previous positron lifetime experiments performed on electrodeposited material have shown that there are no monovacancy defects on the Ba/K sublattice [14].

Magnetization measurements and Laue-back-reflection x-ray photography were used to assess sample quality. Two samples were selected, each with a superconducting onset temperature of 30.6 K and transition widths (ΔT_c) of 3 and 7 K for the smaller (2 mm × 2 mm) and larger (2 mm × 4 mm) crystals, respectively. The larger crystal had more smearing in the Laue patterns, and the broader transition width is probably due to slight variations in the Ba/K ratio across the crystal. The mosaic spread of each sample was less than 1° from the surface normal.

Positron ACAR experiments were performed by attaching a sample, with a high-vacuum epoxy adhesive, onto two 50 μm tungsten wires. The face of the crystal was aligned using Laue backscattering to within 0.5° with respect to the ⟨100⟩ directions and was then mounted in the 2D-ACAR spectrometer with the [001] direction parallel to the center line of the detector system. All measurements were performed to a high level of statistical precision ($\approx 1.2 \times 10^8$ counts) at room temperature and at a pressure of 10^{-8} torr. The spectra were accumulated on a 256 × 256 matrix consisting of 0.143 × 0.143 mrad

0031-9007/94/73(9)/1271(4)$06.00

cells. The angular resolution of the system was 0.5 mrad (3.86 mrad = 1 $Å^{-1}$), including the effects of thermal motion of the positron. A spectrum from bare tungsten wires was also obtained, and background contributions to the experimental spectra were partially accounted for by subtracting this bare wire spectrum ($\approx$12% of the total data).

In defect-free material, positrons assume Bloch states as they enter the lattice. The electron and positron wave functions can change markedly across the unit cell, resulting in variations in electron-positron momentum density due to the overlap of these wave functions. The 2D-ACAR technique correlates Fermi surface features to discontinuities in the electron-positron momentum density. Any Fermi surface related structures, which occur at points in momentum space where electron bands change from occupied to unoccupied states, are overlaid upon the stronger wave-function effects. The strength of the wave-function effects requires that knowledge gained from calculations be used to distinguish these contributions, lest they be confused with Fermi surface related features. Theory also suggests regions in momentum space where Fermi surface features are likely to occur.

Experimental electron-positron momentum spectra include wave-function effects, Fermi surface features, and impurity, defect, and background contributions. These combined spectra are largely isotropic and require further data reduction to identify relevant structures. Two standard analysis procedures are used to investigate features of the experimental spectra. First, a true momentum space sampling can be performed by obtaining the residual spectrum after subtracting an average isotropic spectrum from the raw data. This anisotropic residual enables identification of major electron-positron wave-function effects but may not reveal features with crystal symmetry, such as the Fermi surface. To examine features which may develop in crystal momentum space, the momentum density is reduced to a single Brillouin zone by summing data in higher zones back into the first zone. This Lock-Crisp-West (LCW) zone-folding [15] technique was used to isolate the Fermi surface features, since it averages over the wave-function effects but enhances the Fermi surface breaks which are periodic in momentum space and sum together in the folded Brillouin zone.

First-principles LMTO calculations were used to determine the electronic band structure. The calculations were performed for three different phases in the BKBO system: $BaBiO_3$, $KBiO_3$, and $KBaBi_2O_6$. Each calculation assumed a cubic unit cell for all levels of potassium doping. In the metallic phases, calculations reveal a single band near the Fermi energy of bismuth $6s$ and oxygen $2p$ character. The general shape of the energy bands was found to be largely independent of potassium doping, with the shift of the Fermi energy being the most notable effect. This result agrees well with Korringa-Kohn-Rostoker coherent potential approximation band structure calculations [10] which justify the rigid band approximation for BKBO. Rigid band shifts were therefore used on all three calculations to produce Fermi levels consistent with a potassium doping of $x = 0.41$. These three calculations all produce very similar momentum densities.

Once the wave functions for Bloch state electrons and positrons are determined, the momentum density is calculated using the formula

$$\rho_{ep}(p) = \sum_{n,k} \left| \int d^3r \, \Psi^n_{k,\mathrm{el}}(r) \Psi^*_{\mathrm{pos}}(r) e^{ipr} \right|^2 ,$$

where $\Psi^n_{k,\mathrm{el}}(r)$ is the electron wave function, $\Psi_{\mathrm{pos}}(r)$ is the positron wave function, and the sum is taken over all occupied electron states. This procedure includes no enhancement of the momentum due to electron-positron correlation effects. The calculated electron-positron momentum density $\rho_{ep}(p)$ is largely isotropic and is derived primarily from filled electron band contributions. Additional isotropic contributions in the experimental data arise from defects and background components. The residual anisotropic features can contain information related to crystal symmetry, Fermi surfaces, and the positron distribution. The anisotropic residuals are insensitive to background and defect contributions and so provide a convenient format for comparison between theory and experiment. To ensure consistency of anisotropic features, the same procedures are used in the analysis of the theoretical and experimental spectra. The theoretical spectra have also been convoluted with a Gaussian of appropriate width (0.52 mrad) to account for experimental resolution.

Experimental and theoretical anisotropic residuals for the smaller sample are presented in Fig. 1. These spectra reflect the symmetry of the unit cell and demonstrate the convincing correspondence between experiment and calculations. The strongest features in the theory are the dark wave-function related minima at (1.25, 0), which are easily seen in the experimental spectra. In addition to this, the maxima at (2, 0), the low region near (1.5, 1.5), and the cross structure near the zone center (Γ) are identified well in both plots. Some of these features have been observed previously [16], and both of our measured samples exhibit these key features in this momentum representation. These anisotropic residual plots demonstrate that the calculations accurately represent the electronic structure and positron distribution in the lattice and can account for the major electron-positron wave-function variations.

The experimental data also indicate breaks in momentum density associated with Fermi surface features. Unfortunately, these features are too weak, even in the theoretical anisotropic residual, to allow for a clear identification of the Fermi surface in this representation. The strong wave-function effects overshadow the smaller, Fermi surface related variations. For this reason, we employ the LCW zone-folding procedure which enhances periodic features in momentum space and averages over the wave-function effects.

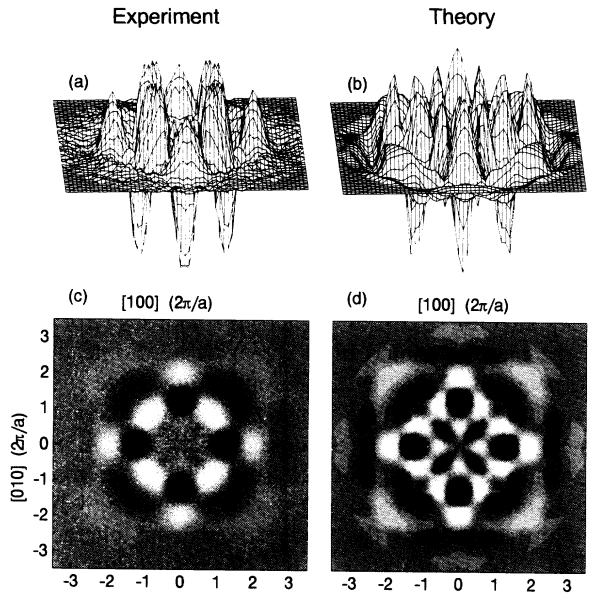

FIG. 1. Experimental and theoretical anisotropic residual distributions for the best quality ($x = 0.41$) BKBO crystal, with dark representing low regions. The theoretical spectrum was obtained from a rigid band shift on the KBa_2BiO_6 supercell calculation. There are strong variations in this true momentum space representation, due to the positron sampling distribution, which are evident in the experiment and reproduced in detail in the LMTO calculations.

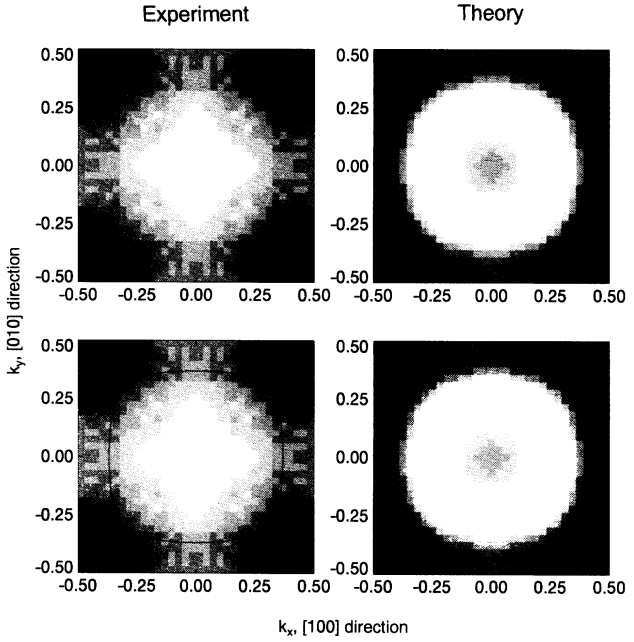

FIG. 2. A gray scale display of the real momentum data from higher order zones combined into a single Brillouin zone using the Lock-Crisp-West technique. The edges of the roughly square Fermi surface can be observed in the measured distribution as well as in the calculations. The shape and location of the measured Fermi break is consistent with that expected from a potassium concentration of $x = 0.4$. The solid line marks the momentum at which the integrated, calculated electron occupancy is at half maximum. Discrepancies between theory and experiment, particularly concerning the zone center (Γ), are addressed in the text.

Experimental and theoretical zone foldings for the smaller sample are presented in Fig. 2. In this single Brillouin zone representation, the depressions at the zone corners and the ridges near X (0.5, 0) are common to both plots. The largest difference between the plots is the peak at Γ in the experimental zone folding, which arises from background contributions and will be discussed later. Most significantly, the experimental data reveal a square Fermi surface feature, with edges roughly midway between Γ and X. The position of this Fermi surface is in excellent agreement with predictions from electronic structure calculations. We have determined, through the close examination of theory and the positron 2D-ACAR experiment, that the Fermi surface in BKBO is a cubic structure, centered around Γ, with rounded corners in the [111] direction. It has flat regions that intersect the vector between Γ and X at roughly 64% of the distance to the zone boundary. Recalling that this experimental technique necessarily integrates the data along the [001] axis, an intensity slice of the folded experimental spectra, presented in Fig. 3, clearly indicates a break in the region of interest, indicative of a Fermi surface. In contrast, an intensity slice taken near the zone edge (inset) reveals no Fermi surface break. This is completely consistent with the expectation of previous electronic structure calculations and with the observation of a similar Fermi surface feature in recent de Haas–van Alphen experiments on BKBO [17]. Figure 3 also indicates the wave-function contribution from filled electron bands and demonstrates clearly that the observed break results from the partially occupied conduction band, as expected for a Fermi surface.

Since the location of the observed Fermi surface in the Brillouin zone is consistent with that predicted by theory, the first-principles band structure calculations provide a clear description of the electronic structure in BKBO. The only significant difference between the experimental zone foldings and those derived from theory is the presence of a peaked feature near Γ in the experimental plots. This feature arises from background contributions due to mounting wires, epoxy, and surface contamination. As previously mentioned, only a subtraction consistent with the counting rates obtained from a bare tungsten wire experiment was performed. Efforts were made to determine the specific lives of background contribution, but other subtractions could not be justified due to the unknown contribution of surface contamination. Regardless, the presence of this background signal centered at Γ does not compromise our ability to resolve the Fermi surface related breaks 64% of the way from Γ

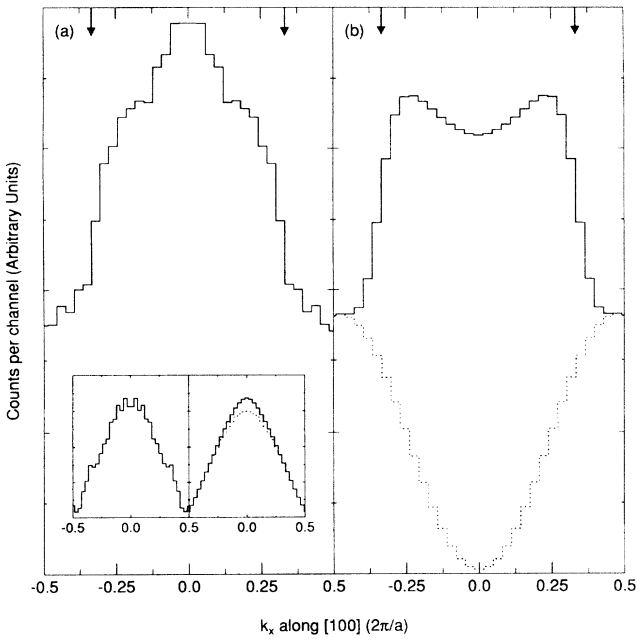

FIG. 3. Linear slice of the single Brillouin zone representation of Fig. 2 for (a) experiment and (b) theory. Slice was prepared by summing over k_y in the range 0.23 to 0.17 and sweeping over k_x. The arrows mark the theoretically predicted position of the break for a potassium doping of $x = 0.4$. Theory plots also show the contribution from the fully occupied bands (dashed line). The inset displays corresponding slices near the zone boundary, summed over k_y in the range 0.5 to 0.44, which reveal no Fermi surface feature. Theoretical calculations have been scaled to experiment in each case. Only the highest quality samples showed evidence of the Fermi surface in our measurements.

to the zone boundary. However, we are not able to identify these breaks in the larger single crystal, in spite of their similar anisotropic residuals. Inhomogeneities in the Ba/K ratio, grain orientation, or degradation of the sample surface may distort these features for the larger crystal, thereby smearing the regions of the breaks. These results indicate that sample quality is a crucial issue for the observation of Fermi surface related structures in BKBO.

By placing a cubic volume inside and outside the observed Fermi surface and accounting for the number of electrons present, we are able to estimate the amount of doping in the crystal. With two electrons per band, a lower bound on the Fermi volume suggests a level of $x = 0.52$, while an upper bound suggests that $x = 0.38$. These values bracket the metallic phases of BKBO very well and provide further justification that the location of the observed Fermi surface breaks are reasonable. Another check on the validity of the result is the sensitivity of the LCW procedure to the lattice parameter. If the cubic lattice parameter is changed by as little as 1%, the Fermi surface features would themselves be averaged over. Since the zone folding depends critically upon the presumed structure and size of the unit cell, our ability to identify the Fermi surface breaks confirms the choice of structural parameters.

The observed large, parallel sheets of Fermi surface in BKBO suggest the presence of effects due to Fermi surface nesting. Incommensurate modulations, consistent with structures that could be explained by these types of symmetry, have been observed in BKBO [18]. Our data alone are not sufficient to distinguish differences in subtle electronic structure features that may arise in some theories. Many models have been developed to explain the existing lattice instabilities in BKBO and the closely related high-T_c cuprates. Some theories even suggest that the superconducting state itself is driven by Fermi surface nesting [19], but a connection between BKBO and the cuprates based upon nesting arguments is not straightforward. Nesting in many p-type cuprates is two dimensional in nature, which is quite different from the three-dimensional character of BKBO. The significance of this dimensionality in issues such as quasiparticle scattering and the superconducting order parameter still requires investigation. Nonetheless, the similarities in high transition temperature, presence of lattice instabilities, and now the direct identification of strongly nested Fermi surface regions all suggest analogous mechanisms in these oxide materials.

This work was performed under the auspices of the U.S. Department of Energy by Lawrence Livermore National Laboratory under Contract No. W-7405-ENG-48 and supported by the National Science Foundation Grant No. DMR-90-21029.

[1] H. Haghighi *et al.*, Phys. Rev. Lett. **67**, 382 (1991).
[2] P. A. Sterne *et al.*, J. Chem. Phys. Solids **54**, 1231 (1993).
[3] R. H. Howell *et al.*, Phys. Rev. B **49**, 13 127 (1994).
[4] M. Peter *et al.*, Europhys. Lett. **18**, 313 (1992).
[5] L. C. Smedskjaer *et al.*, Physica (Amsterdam) **192C**, 259 (1992).
[6] C. G. Olson *et al.*, Phys. Rev. B **42**, 381 (1990).
[7] D. S. Dessau *et al.*, Phys. Rev. Lett. **71**, 2781 (1993).
[8] L. F. Mattheis, E. M. Gyorgy, and D. M. Johnson, Phys. Rev. B **37**, 3745 (1988).
[9] D. G. Hinks *et al.*, Nature (London) **333**, 836 (1988).
[10] A. Barbieri *et al.*, Key. Engr. Mat. **48**, 101 (1990).
[11] W. D. Mosley *et al.*, J. Cryst. Growth **128**, 804 (1993).
[12] M. L. Norton, Mater. Res. Bull. **24**, 1391 (1989).
[13] S. Y. Pei *et al.*, Phys. Rev. B **41**, 4126 (1990).
[14] W. D. Mosley *et al.*, Phys. Rev. B **48**, 611 (1993).
[15] D. G. Lock, V. H. C. Crisp, and R. N. West, J. Phys. F **30**, 389 (1973).
[16] L. C. Smedskjaer (private communication).
[17] R. G. Goodrich *et al.*, J. Phys. Chem. Solids **54**, 1251 (1993).
[18] M. Verwerft *et al.*, Phys. Rev. B **44**, 9547 (1991).
[19] A. Virosztek and J. Ruvalds, Phys. Rev. B **42**, 4064 (1990).

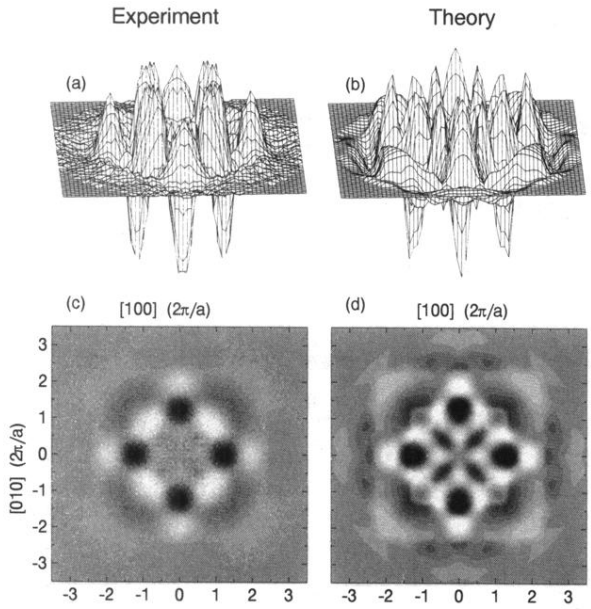

FIG. 1. Experimental and theoretical anisotropic residual distributions for the best quality ($x = 0.41$) BKBO crystal, with dark representing low regions. The theoretical spectrum was obtained from a rigid band shift on the KBa_2BiO_6 supercell calculation. There are strong variations in this true momentum space representation, due to the positron sampling distribution, which are evident in the experiment and reproduced in detail in the LMTO calculations.

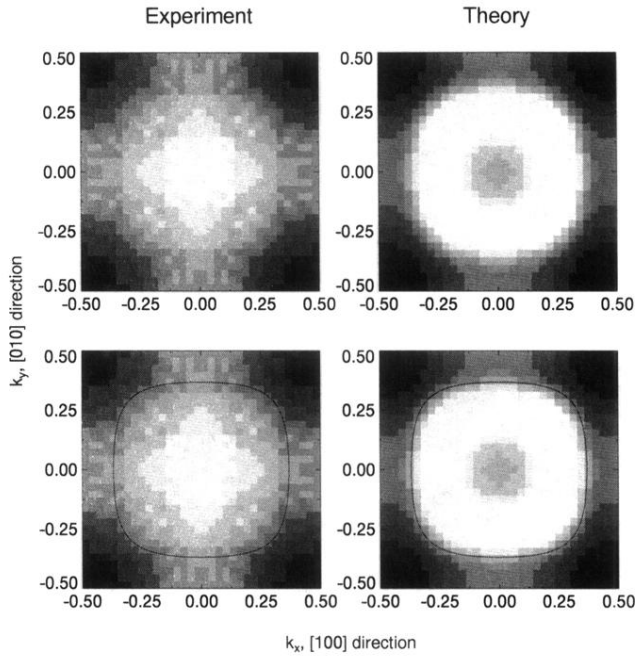

FIG. 2. A gray scale display of the real momentum data from higher order zones combined into a single Brillouin zone using the Lock-Crisp-West technique. The edges of the roughly square Fermi surface can be observed in the measured distribution as well as in the calculations. The shape and location of the measured Fermi break is consistent with that expected from a potassium concentration of $x = 0.4$. The solid line marks the momentum at which the integrated, calculated electron occupancy is at half maximum. Discrepancies between theory and experiment, particularly concerning the zone center (Γ), are addressed in the text.